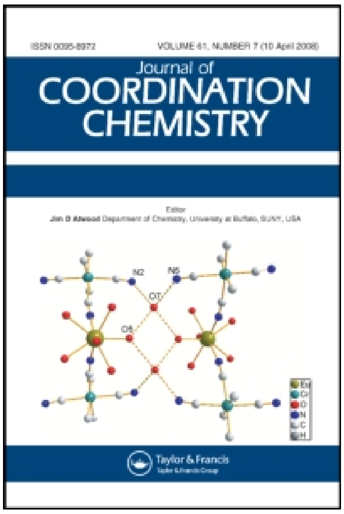

Journal of Coordination Chemistry
Publication details, including instructions for authors and subscription information:
http://www.informaworld.com/smpp/title~content=t713455674

LIGAND SUBSTITUTION ON $HRu_3(\mu\text{-}NC_5H_3CO_2Me)(CO)_{10}$ AND $H_2Ru_3(\mu\text{-}NC_5H_3CO_2Me)_2(CO)_8$. CRYSTAL STRUCTURES OF $(\mu\text{-}H)Ru_3(\mu\text{-}\eta^2\text{-}NC5H_3CO_2Me)(CO)_9(PPh_3)$AND $(\mu\text{-}H)_2Ru_3(\mu\text{-}\eta^2\text{-}NC_5H_3CO_2Me)_2(CO)_7(PPh_3)$*

Melvyn Rowen Churchill[a]; Robert Hall[a]; Charles H. Lake[a]; Laurence M. Toomey[a]; Jerome B. Keister[a]
[a] Department of Chemistry, University at Buffalo, State University of New York, Buffalo, NY, USA

To cite this Article Churchill, Melvyn Rowen , Hall, Robert , Lake, Charles H. , Toomey, Laurence M. and Keister, Jerome B.(1999) 'LIGAND SUBSTITUTION ON $HRu_3(\mu\text{-}NC_5H_3CO_2Me)(CO)_{10}$ AND $H_2Ru_3(\mu\text{-}NC_5H_3CO_2Me)_2(CO)_8$. CRYSTAL STRUCTURES OF $(\mu\text{-}H)Ru_3(\mu\text{-}\eta^2\text{-}NC5H_3CO_2Me)(CO)_9(PPh_3)$AND $(\mu\text{-}H)_2Ru_3(\mu\text{-}\eta^2\text{-}NC_5H_3CO_2Me)_2(CO)_7(PPh_3)$*', Journal of Coordination Chemistry, 47: 2, 211 — 229

To link to this Article: DOI: 10.1080/00958979908023055

URL: http://dx.doi.org/10.1080/00958979908023055

J. Coord. Chem., 1999, Vol. 47, pp. 211–229
Reprints available directly from the publisher
Photocopying permitted by license only

LIGAND SUBSTITUTION ON $HRu_3(\mu\text{-}NC_5H_3CO_2Me)(CO)_{10}$ AND $H_2Ru_3(\mu\text{-}NC_5H_3CO_2Me)_2(CO)_8$. CRYSTAL STRUCTURES OF $(\mu\text{-}H)Ru_3(\mu\text{-}\eta^2\text{-}NC_5H_3CO_2Me)(CO)_9(PPh_3)$ AND $(\mu\text{-}H)_2Ru_3(\mu\text{-}\eta^2\text{-}NC_5H_3CO_2Me)_2(CO)_7(PPh_3)$*

MELVYN ROWEN CHURCHILL, ROBERT HALL,
CHARLES H. LAKE, LAURENCE M. TOOMEY
and JEROME B. KEISTER[†]

*Department of Chemistry, University at Buffalo, State University of New York,
Buffalo, NY 14260-3000, USA*

(Received 24 March 1998; Revised 24 April 1998; In final form 25 June 1998)

Clusters of the series $HRu_3(\mu\text{-}NC_5H_3CO_2Me)(CO)_{10-n}(PPh_3)_n$ ($n = 0, 1$) and $H_2Ru_3(\mu\text{-}NC_5H_3CO_2Me)_2(CO)_{8-n}(PPh_3)_n$ ($n = 0, 1$) have been prepared. X-ray crystallographic studies of $HRu_3(\mu\text{-}NC_5H_3\text{-}5\text{-}CO_2Me)(CO)_9(PPh_3)$ and $H_2Ru_3(\mu\text{-}NC_5H_3\text{-}5\text{-}CO_2Me)_2(CO)_7(PPh_3)$ have been performed. The regiochemistry of PPh_3 substitution in both is consistent with greater *cis* labilization by the N-donor atom compared with the C-donor atom of the nicotinyl ligand.

The monohydrido-methyl nicotinate derivative, $(\mu\text{-}H)Ru_3(\mu\text{-}\eta^2\text{-}NC_5H_3CO_2Me)(CO)_9(PPh_3)$, crystallizes in the orthorhombic space group Pbca (No. 61) with $a = 22.891(3)$, $b = 12.641(1)$, $c = 24.694(3)$ Å, $V = 7145.6(14)$ Å^3 and $Z = 8$. The structure was solved and refined to $R = 2.60\%$ for 2191 data with $|F_0| \geq 6\sigma(F_0)$. The Ru_3 triangle has interatomic distances (in increasing order) of Ru(1)–Ru(3) = 2.854(1), Ru(2)–Ru(3) = 2.861(1) and Ru(1)–Ru(2) = 2.910(1) Å.

---

* Structural studies on ruthenium carbonyl hydrides. Part 20. For recent previous parts see the following: (a) This paper should be considered Part 19. W. Paw, C.H. Lake, M.R. Churchill and J.B. Keister, *Organometallics*, **14** (1995) 3768–3782. (b) Part 18. M.R. Churchill, C.H. Lake, R.A. Lashewycz-Rubycz, H. Yao, R. McCargar and J.B. Keister, *J. Organomet. Chem.*, **452** (1993) 151–160. (c) Part 17. M.R. Churchill, C.H. Lake, F.J. Safarowic, D.S. Parfitt, L.R. Nevinger and J.B. Keister, *Organometallics*, **12** (1993) 671–679. (d) Part 16. M.R. Churchill, C.H. Lake, W.G. Feighery and J.B. Keister, *Organometallics*, **10** (1991) 2384–2391. (e) Part 15. M.R. Churchill, L.A. Buttrey, J.B. Keister, J.W. Ziller, T.S. Janik and W.S. Striejewske, *Organometallics*, **9** (1990) 766–773.

[†] Corresponding author. E-mail: keister@acsu.buffalo.edu.

The nicotinate ligand bridges the cluster through axial sites on Ru(1) and Ru(2), with Ru(1)–N(1) = 2.136(6) Å and Ru(2)–C(41) = 2.088(7) Å; the μ-hydride ligand (which was located and refined) also bridges the Ru(1)–Ru(2) edge, in a diequatorial location, with Ru(1)–H(1) = 1.69(5) Å, Ru(2)–H(1) = 1.72(5) Å and ∠Ru(1)–H(1)–Ru(2) = 117.5(27)°. The PPh_3 ligand occupies an equatorial site on Ru(1), with Ru(1)–P(1) = 2.365(2) Å and ∠Ru(2)–Ru(1)–P(1) = 111.5(1)°.

The dihydrido-bis(methyl nicotinate) derivative, $(\mu\text{-}H)_2Ru_3(\mu\text{-}\eta^2\text{-}NC_5H_3\text{-}5\text{-}CO_2Me)_2(CO)_7(PPh_3)$, crystallizes in the monoclinic space group $P2_1/c$ (No. 14) with $a = 12.104(4)$, $b = 27.810(7)$, $c = 12.290(3)$ Å, $\beta = 96.55(2)°$, $V = 4110(2)$ Å^3 and $Z = 4$. The structure was refined to $R = 7.96\%$ for those 2761 reflections with $|F_0| > 3\sigma(F_0)$. Distances within the Ru_3 triangle are (in increasing order) Ru(2)–Ru(3) = 2.846(2), Ru(1)–Ru(3) = 2.914(2) and Ru(1)–Ru(2) = 2.924(2) Å. The nicotinate ligands are involved in diaxial bridges across Ru(1)–Ru(2) (with Ru(1)–N(51) = 2.122(13) and Ru(2)–C(52) = 2.100(16) Å) and Ru(1)–Ru(3) (with Ru(3)–N(61) = 2.129(14) and Ru(1)–C(62) = 2.053(16) Å) in such a way that N(51) lies *trans* to C(62) on Ru(1) with ∠N(51)–Ru(1)–C(62) = 161.5(6)°. Hydride ligands bridge the Ru(1)–Ru(2) and Ru(1)–Ru(3) bonds, while the PPh_3 ligand occupies an equatorial site on Ru(3), with Ru(3)–P(1) = 2.379(4) Å.

Keywords: Triruthenium; ligand substitution; structures; triphenylphosphine

INTRODUCTION

Reactions of nitrogen heterocycles with transition metal clusters have been studied by a number of workers.[1] Metallation of C–H bonds is commonly observed.[2–7] These reactions have been suggested as models for denitrogenation catalysis.[8]

We were interested in preparing metal clusters containing electroactive organic ligands. Since the electrochemistry of surface adsorbed nicotinic acid is well-characterized, we had hoped to prepare clusters containing nicotinic acid derivatives and in a variety of coordination geometries. This paper concerns complexes derived from methyl nicotinate.

EXPERIMENTAL

General $Ru_3(CO)_{12}$ was prepared as previously described.[9] Methyl nicotinate and trimethylamine-N-oxide dihydrate were purchased from Aldrich Chemical and were used as received. All reactions were carried out under nitrogen utilizing standard Schlenk line techniques. Purification was done by thin layer chromatography on silica gel with dichloromethane : heptane as eluent. Recrystallization was done using methanol/dichloromethane. Infrared spectra were recorded on a Nicolet 550 FT-IR Spectrophotometer. The ^1H NMR spectra were recorded on Varian Gemini 300 or VXR-400 instruments in deuterochloroform with TMS as reference. The ^{31}P NMR spectra were obtained on a VXR-400 instrument in deuterochloroform with chemical shifts referenced to o-phosphoric acid. All ^{1}H and ^{31}P data were obtained at room temperature, unless otherwise stated.

$HRu_3(\mu\text{-}NC_5H_3CO_2Me)(CO)_{10}$ (**1**) Ru_3CO_{12} (106 mg, 0.166 mmol) and methyl nicotinate (78.9 mg, 0.711 mmol) were dissolved in 50 mL of heptane in a 125-mL round-bottomed flask. The solution was then heated under a stream of nitrogen at 75–80°C for about 10 h. The products were purified using TLC on silica gel with a 60 : 40 mixture of dichloromethane : heptane (v : v) as eluent. A single yellow band was eluted and extracted with dichloromethane. The yield is 39.6 mg (34.7%). ^{1}H NMR ($CDCl_3$): −14.50 (s, 1H), 3.90 (s, 3H), 7.45 (d, 1H, $J_{HH} = 6.0$ Hz), 7.70 (d, 1H, $J_{HH} = 6.0$ Hz), 8.55 (s, 1H) ppm. IR (cyclohexane): 2063 s, 2050 s, 2026 s, 2013 s, 2001 s cm^{-1}.

$HRu_3(\mu\text{-}NC_5H_3CO_2Me)(CO)_9(PPh_3)$ (**2**)
(**1**) (77 mg, 0.107 mmol) and PPh_3 (31.8 mg, 0.121 mmol) were dissolved in 50 mL of heptane in a 125-mL round-bottomed flask. The solution was heated under nitrogen for 1–2 h at 65°C. The solution was evaporated to dryness under vacuum. Products were separated by TLC on silica gel using a 93 : 7 mixture of dichloromethane : heptane (v : v) as eluent. Two bands were extracted with dichloromethane. The upper band was identified as (**2**) (40.2% yield). Extraction of the second band gave a product (29.7 mg) which showed no hydride resonances in the ^{1}H NMR spectrum. No further identification of this product was made.

$HRu_3(NC_5H_3CO_2Me)(CO)_9(PPh_3)$ (**2**): IR (hexane): 2084 m, 2061 m, 2054 s, 2045 s, 2009 s, 1992 m, 1978 m, 1957 m, 1738 m cm^{-1}. ^{1}H NMR ($CDCl_3$): −14.32 (d, 1H, $J_{PH} = 11.9$ Hz), 3.90 (s, 3H), 7.4 (m, 18H) ppm. ^{31}P NMR ($CDCl_3$): 33.8 (s) ppm. EI-MS *m*/*z* 956 ($^{102}Ru_3$).

$H_2Ru_3(NC_5H_3CO_2Me)_2(CO)_8$ (**3**)
$Ru_3(CO)_{12}$ (206.5 mg, 0.323 mmol) and methyl nicotinate (129.7 mg, 1.17 mmol) were dissolved in 60 mL of heptane in a 125-mL Schlenk flask. The solution was refluxed under nitrogen for 3 h. The solution was then concentrated under vacuum. Purification was obtained by thin layer chromatography on silica gel, using a 60 : 40 mixture of dichloromethane : heptane (v : v) as eluent. The two bands found were identified as (**1**) (7 mg, 3.8% yield), and (**3**) (187 mg, 72.2% yield).

$H_2Ru_3(NC_5H_3CO_2Me)_2(CO)_8$ (**3**): IR (hexane): 2051 s, 2044 s, 2009 s, 2006 s, 1989 s cm^{-1}. ^{1}H NMR ($CDCl_3$): −13.18 (s, 1H), −12.18 (s, 1H), 3.75 (s, 3H), 3.85 (s, 3H), 7.50 (d, $J_{HH} = 8$ Hz, 1H), 7.55 (d, $J_{HH} = 8$ Hz, 1H), 7.73 (dd, $J_{HH}=4$ and 1.5 Hz, 1H), 7.77 (dd, $J_{HH}=4$ and 1.5 Hz, 1H), 8.64 (d, $J_{HH}=1.5$ Hz, 1H), 8.72 (d, $J_{HH}=1.5$ Hz, 1H) ppm. EI-MS *m*/*z* 803 ($^{102}Ru_3$).

$H_2Ru_3(NC_5H_3CO_2Me)_2(CO)_7(PPh_3)$ (**4**)

(**3**) (75 mg, 0.094 mmol) and PPh_3 (20 mg, 0.076 mmol) were dissolved in 50 mL of heptane in a 125-mL round-bottomed flask. The solution was heated under nitrogen at 70°C for 1–2 h. The solution was evaporated to dryness, then the residue dissolved into a small amount of dichloromethane, and applied to preparative TLC plates and eluted with a 50 : 50 mixture of dichloromethane:heptane (v : v). (**4**) is the only band isolated. The yield was 34.5 mg (35.7%).

$H_2Ru_3(NC_5H_3CO_2Me)_2(CO)_7(PPh_3)$ (**4**): IR (hexane): 2062 s, 2038 s, 2007 s, 2000 s, 1978 s, 1957 s, 1735 s cm^{-1}. ^{1}H NMR($CDCl_3$): −11.95 (d, 1H, $J_{PH}=11.4$ Hz), −12.91 (d, 1H, $J_{HH}=4.4$ Hz), 3.76 (s, 3H), 3.97 (s, 3H), 7.5 (m, 20H), 8.70 (s, 1H) ppm. ^{31}P NMR ($CDCl_3$): 35.7 (s) ppm. EI-MS *m*/*z* 1035 ($^{102}Ru_3$).

$H_2Ru_3(NC_5H_3CO_2Me)_2(CO)_6(PPh_3)_2$ (**5**)

$H_2Ru_3(NC_5H_3CO_2Me)_2$ $(CO)_7(PPh_3)$ (**4**) (72.7 mg, 0.072 mmol) and PPh_3 (18.7 mg, 0.0714 mmol) were dissolved in 50 mL of THF in a 125-mL round-bottomed flask. Another solution of 8.3 mg (0.0748 mmol) of trimethylamine-N-oxide dihydrate in 20 mL of acetonitrile was also prepared. The acetonitrile solution was slowly added dropwise to the THF solution over 5 min. The flask was then sealed, and stirred for 1–2 h with a stream of nitrogen flowing over it. The resultant solution was evaporated to dryness, and the residue dissolved in minimum of CH_2Cl_2. It was then separated by TLC (silica gel), using a 95 : 5 mixture of CH_2Cl_2 : heptane as elutent. The first band isolated (< 2.0%) was identified as **3** by the IR and ^{1}H NMR spectra. The second band (47.1 mg, 53.0% yield) was identified as $H_2Ru_3(NC_5H_3CO_2Me)_2$ $(CO)_6(PPh_3)_2$ (**5**). The third and fourth bands comprised together 29.3 mg; these products were not fully characterized.

$H_2Ru_3(\mu\text{-}NC_5H_3CO_2Me)_2(CO)_6(PPh_3)_2$ (**5**): ^{1}H NMR ($CDCl_3$): −12.55 (dd, 1H, $J_{PH}=2.0$, 12.0 Hz), −11.79 (dd, 1H, $J_{PH}=1.6$, 10.8 Hz), 3.75 (s, 3H), 3.93 (s, 3H), 6.96 (d, 1H, $J_{HH}=4.0$ Hz), 7.2 (m, 34H), 7.7 (br s, 1H), 8.4 (br s, 1H) ppm. ^{31}P NMR ($CDCl_3$): 32.7 (d, 1P, $J_{PP}=16.0$ Hz), 39.2 (d, 1P, $J_{PP}=16.0$ Hz) ppm. IR (hexane): 2050 m, 2031 m, 2018 s, 1981 s, 1970 s, 1959 s, 1734 s cm^{-1}. EI-MS *m*/*z* 1271 ($^{102}Ru_3$).

Collection of X-Ray diffraction data for $(\mu\text{-}H)Ru_3(\mu\text{-}\eta^2\text{-}NC_5H_3CO_2Me)$ $(CO)_9(PPh_3)$ (**2**) A crystal of approximate dimensions 0.23 × 0.17 × 0.17 mm was selected for the diffraction study. It was sealed in a

0.2 mm-diameter thin-walled capillary, mounted on a eucentric goniometer and centered on a Siemens R3m/V automated four-circle diffractometer. Set-up operations were carried out as described previously.[10] The crystal belongs to the orthorhombic system (mmm or D_{2h} diffraction symmetry); the systematic absences $0k\ell$ for $k = 2n + 1$, $h0\ell$ for $\ell = 2n + 1$ and $hk0$ for $h = 2n + 1$ uniquely define the centrosymmetric orthorhombic space group Pbca (No. 61). A total of 7294 reflections, representing two equivalent forms of data ($hk\ell$, $hk\bar{\ell}$) were collected by means of an ω-scan technique, corrected for Lorentz and polarization factors and for the effects of absorption, and were averaged ($R(\mathrm{int}) = 1.81\%$), yielding 3335 reflections, of which 2191 (65.7%) had $|F_0| > 6\sigma(F_0)$. Details of data collection appear in Table I.

Solution and refinement of the crystal structure of $(\mu\text{-}H)Ru_3(\mu\text{-}\eta^2\text{-}NC_5H_3CO_2Me)(CO)_9(PPh_3)$ (**2**)

All crystallographic calculations were carried out with the Siemens SHELXTL PLUS program package[11] on a VAX station 3100 computer. The analytical scattering factors for neutral atoms were corrected for both components ($\Delta f'$ and $i\Delta''$) of anomalous dispersion.[12] The phase problem was solved by direct methods and the structural analysis was completed by a combination of difference-Fourier syntheses and least-squares refinement. Positional and anisotropic thermal parameters for all non-hydrogen atoms were refined. The hydrogen atom of the μ-hydride ligand was located directly; its positional parameters and isotropic thermal parameter were also included in the refinement process. All organic hydrogen atoms were placed at calculated positions with $d(\mathrm{C{-}H}) = 0.96$ Å.[13]

The refinement process converged [$\Delta/\sigma(\max) = 0.003$] with $R(F) = 2.60\%$ and $R(wF) = 2.23\%$ for those 2191 reflections with $|F_0| > 6\sigma(F_0)$ and $R(F) = 5.56\%$ and $R(wF) = 3.20\%$ for all 3335 independent reflections. A final difference-Fourier map contained features only in the range -0.61 to $+0.71$ e$^-$/Å^3. Final atomic coordinates are provided in Table II.

Collection of X-ray diffraction data for $(\mu\text{-}H)_2Ru_3(\mu\text{-}\eta^2\text{-}NC_5H_3CO_2Me)_2(CO)_7(PPh_3)$ (**4**) A crystal of approximate dimensions 0.2 × 0.2 × 0.3 mm was selected for the X-ray diffraction study. Data were collected and were processed as in the structural study described above. Details appear in Table I. The crystal belongs to the monoclinic system (2/m or C_{2h} diffraction symmetry); the systematic absences $h0\ell$ for $\ell = 2n + 1$ and $0k0$ for $k = 2n + 1$ uniquely define the centrosymmetric monoclinic space group $P2_1/c$ (No. 14).

TABLE I Details on the data collection for the X-ray diffraction studies

	$HRu_3(NC_5H_3CO_2Me)$ $(CO)_9(PPh_3)$	$H_2Ru_3(NC_5H_3CO_2Me)_2$ $(CO)_7(PPh_3)$
Formula	$C_{34}H_{22}NO_{11}PRu_3$	$C_{39}H_{29}N_2O_{11}PRu_3$
Crystal system	Orthorhombic	Monoclinic
Space group	Pbca (No. 61)	$P2_1/c$ (No. 14)
a, Å	22.891(3)	12.104(4)
b, Å	12.641(1)	27.810(7)
c, Å	24.694(3)	12.290(3)
β, deg	90.000	96.55(2)
V, Å^3	7145.6(14)	4110(2)
T, °C	25	23
Z	8	4
Molecular weight	954.7	1035.8
Density, g/cm^3	1.775	1.674
μ, mm^{-1}	1.330	1.163
T_{min}/T_{max}	0.682/0.699	0.743/0.870
2θ range	5.0–40.0	5.0–45.0
Index ranges	h 0–22	h 0–13
	k 0–12	k 0–30
	ℓ −23 to 23	ℓ −13 to 13
Reflections collected	7294	5958
Independent reflections	3335	5383
Reflections used	2191 ($F > 6\sigma(F)$)	2761 ($F > 3\sigma(F)$)
Final R indices	$R(F) = 2.60\%$	$R(F) = 7.96\%$
	$R(wF) = 3.02\%$	$R(wF) = 3.20\%$
Goodness of fit	1.00	1.47
Largest diff. peak, e$^-$/Å^3	0.71	0.87
Largest diff. "hole", e$^-$/Å^3	−0.61	−0.83

TABLE II Final atomic coordinates ($\times 10^4$) and equivalent isotropic displacement coefficients (Å^2 $\times$ 10^3) for $(\mu\text{-H})Ru_3(\mu\text{-}\eta^2\text{-}NC_5H_3CO_2Me)(CO)_9(PPh_3)$

	x	y	z	U(eq)
Ru(1)	660(1)	1272(1)	1288(1)	30(1)
Ru(2)	1754(1)	1357(1)	1887(1)	37(1)
Ru(3)	958(1)	−364(1)	2035(1)	39(1)
H(1)	1154(22)	2000(37)	1631(20)	29(16)
P(1)	486(1)	2864(2)	812(1)	34(1)
O(1)	−79(3)	−263(5)	658(2)	66(2)
O(2)	−312(3)	1844(4)	2053(2)	65(2)
O(3)	1529(3)	2568(5)	2947(2)	93(3)
O(4)	2696(3)	−62(5)	2361(3)	94(3)
O(5)	2531(3)	3160(6)	1522(3)	112(4)
O(6)	525(3)	931(5)	3004(2)	75(3)
O(7)	1343(3)	−1468(4)	986(2)	68(3)
O(8)	−197(3)	−1547(5)	1987(3)	84(3)
O(9)	1671(3)	−1860(5)	2752(3)	104(3)
O(10)	1412(3)	54(4)	−816(2)	60(2)
O(11)	2382(3)	−65(5)	−825(2)	79(3)
N(1)	1384(2)	839(4)	788(2)	30(2)

TABLE II (*Continued*)

	x	y	z	U(eq)
C(1)	177(3)	351(6)	902(3)	39(3)
C(2)	63(3)	1613(6)	1767(3)	43(3)
C(3)	1590(3)	2074(7)	2578(4)	53(3)
C(4)	2337(4)	457(7)	2174(3)	61(4)
C(5)	2241(4)	2490(7)	1669(3)	55(3)
C(6)	704(3)	494(7)	2634(3)	53(3)
C(7)	1225(3)	−1010(6)	1365(3)	45(3)
C(8)	240(4)	−1107(6)	2006(3)	50(3)
C(9)	1389(4)	−1290(7)	2501(4)	65(4)
C(11)	−290(3)	3077(6)	663(3)	36(3)
C(12)	−604(4)	2328(6)	376(3)	55(4)
C(13)	−1194(4)	2437(7)	299(3)	61(4)
C(14)	−1486(4)	3281(8)	513(4)	67(4)
C(15)	−1181(4)	4040(7)	787(4)	81(5)
C(16)	−590(3)	3944(6)	860(3)	53(4)
C(21)	703(3)	4102(5)	1141(3)	32(3)
C(22)	795(3)	5005(6)	837(3)	52(3)
C(23)	933(4)	5956(6)	1088(4)	63(4)
C(24)	982(4)	6004(7)	1634(4)	68(4)
C(25)	885(3)	5120(7)	1945(3)	59(4)
C(26)	752(3)	4178(6)	1699(3)	46(3)
C(31)	880(4)	2951(5)	171(3)	37(3)
C(32)	628(4)	2857(6)	−338(3)	59(4)
C(33)	989(6)	2850(7)	−792(4)	78(5)
C(34)	1579(6)	2938(7)	−739(4)	87(5)
C(35)	1827(4)	3052(6)	−244(4)	61(4)
C(36)	1481(4)	3043(5)	208(3)	49(3)
C(41)	1874(3)	820(5)	1095(3)	33(3)
C(42)	2402(3)	541(6)	846(3)	40(3)
C(43)	2421(3)	289(6)	314(3)	43(3)
C(44)	1910(3)	313(6)	4(3)	38(3)
C(45)	1402(3)	594(5)	257(3)	35(3)
C(46)	1927(4)	81(6)	−586(3)	49(4)
C(47)	1415(4)	−153(8)	−1387(3)	99(5)

Solution and refinement of the crystal structure of $(\mu\text{-}H)_2Ru_3(\mu\text{-}\eta^2\text{-}NC_5H_3CO_2Me)_2(CO)_7(PPh_3)$ Solution of the structure was carried out as described above. It should be noted that the set of diffraction data for this complex was rather weak. Of 5383 independent reflections, only 2761 (51.3%) had $|F_0| > 3\sigma(F)$. Convergence was reached with $R(F) = 7.96\%$ and $R(wF) = 3.19\%$ for the data with $|F_0| > 3\sigma(F)$. The two μ-hydride ligands were located from difference-Fourier syntheses but were not well-behaved upon refinement; the reported coordinates are those derived from the difference-Fourier peaks. All organic hydrogens were placed in idealized locations. A final difference-Fourier map showed features only in the range -0.83 to $+0.87\,e^-/\text{Å}^3$; the structure is thus both correct and complete. Final positional parameters are collected in Table III.

TABLE III Final atomic coordinates ($\times 10^4$) and equivalent isotropic displacement coefficients ($\text{Å}^2 \times 10^3$) for $(\mu\text{-H})_2\text{Ru}_3(\mu\text{-}\eta^2\text{-NC}_5\text{H}_3\text{Me})_2(\text{CO})_7(\text{PPh}_3)$

	x	*y*	*z*	*U* (eq)
Ru(1)	1638(1)	790(1)	1677(1)	44(1)
Ru(2)	2336(1)	1541(1)	3275(1)	55(1)
Ru(3)	128(1)	1552(1)	2193(1)	47(1)
H(1)	842	1221	1172	40
H(2)	2226	883	2754	40
O(1)	3208(11)	-50(5)	2026(12)	98(7)
O(2)	590(10)	398(4)	-474(9)	79(6)
O(3)	4687(11)	1393(6)	4323(11)	117(8)
O(4)	2138(12)	2615(4)	3636(11)	98(7)
O(5)	1134(11)	1267(5)	5260(9)	92(7)
O(6)	844(10)	2461(4)	1184(10)	74(6)
O(7)	-697(12)	2118(5)	4054(11)	105(8)
C(1)	2600(14)	276(6)	1921(14)	57(8)
C(2)	990(14)	550(6)	366(13)	53(5)
C(3)	3740(16)	1439(8)	3948(14)	74(10)
C(4)	2226(17)	2205(6)	3498(15)	69(9)
C(5)	1571(16)	1365(6)	4526(14)	62(9)
C(6)	586(15)	2098(6)	1594(16)	66(9)
C(7)	-394(15)	1905(7)	3335(15)	62(9)
P(1)	-1516(4)	1512(2)	936(3)	46(2)
C(21)	-1301(16)	1418(6)	-478(13)	50(8)
C(22)	-386(15)	1601(6)	-885(14)	61(8)
C(23)	-209(16)	1560(7)	-1955(16)	80(10)
C(24)	-1005(19)	1342(8)	-2700(20)	89(12)
C(25)	-1938(21)	1174(8)	-2339(18)	103(13)
C(26)	-2109(16)	1200(6)	-1230(15)	60(8)
C(31)	-2510(17)	1023(8)	1144(14)	49(9)
C(32)	-2204(16)	556(8)	1082(13)	61(9)
C(33)	-2962(19)	196(7)	1263(16)	74(10)
C(34)	-3920(19)	279(9)	1526(21)	115(14)
C(35)	-4246(18)	744(9)	1669(16)	104(12)
C(36)	-3577(20)	1138(7)	1455(16)	87(11)
C(41)	-2331(14)	2062(6)	896(15)	49(8)
C(42)	-2656(17)	2253(7)	1843(16)	93(11)
C(43)	-3320(17)	2664(9)	1832(18)	103(12)
C(44)	-3557(17)	2913(7)	875(19)	85(11)
C(45)	-3238(18)	2724(7)	-34(16)	90(11)
C(46)	-2652(16)	2312(7)	-32(14)	71(10)
N(51)	2760(10)	1277(4)	1053(11)	46(6)
O(51)	4780(13)	1924(6)	-1716(11)	123(9)
O(52)	3896(14)	1218(6)	-1890(12)	129(9)
C(52)	3029(13)	1648(6)	1803(12)	43(7)
C(53)	3716(15)	2004(6)	1476(16)	72(10)
C(54)	4132(15)	2012(7)	487(18)	77(10)
C(55)	3851(15)	1616(7)	-260(14)	60(9)
C(56)	3181(15)	1263(6)	66(13)	55(8)
C(57)	4235(18)	1622(10)	-1343(16)	84(12)
C(58)	4167(17)	1194(7)	-2953(16)	207(18)
N(61)	-202(12)	871(5)	2879(10)	45(6)
O(61)	-2527(15)	-215(6)	4579(14)	118(9)
O(62)	-2698(13)	562(6)	4769(13)	106(8)

TABLE III (*Continued*)

	x	y	z	U(eq)
C(62)	446(13)	513(6)	2560(12)	38(7)
C(63)	249(15)	49(7)	2907(13)	57(9)
C(64)	−553(17)	−56(7)	3535(15)	71(10)
C(65)	−1235(15)	306(8)	3832(14)	53(9)
C(66)	−982(14)	772(7)	3519(13)	50(8)
C(67)	−2198(21)	195(10)	4446(20)	90(14)
C(68)	−3714(17)	354(10)	5181(17)	275(26)

RESULTS AND DISCUSSION

Reactions of 3-substituted pyridines with $Ru_3(CO)_{12}$ have been shown previously to give products metallated at the 2- and 5-positions, with the latter preferred. As the carbonyl group on methyl nicotinate could change the regiochemistry by O-coordination, we thought that activation of methyl nicotinate at the 2-position might be more favorable. However, only metallation at the 5-position is found for mono- and dinicotinyltriruthenium clusters.

$HRu_3(\mu\text{-}NC_5H_3CO_2Me)(CO)_{10-n}(PPh_3)_n$ ($n = 0$, 1)

The major product of the reaction of Ru_3CO_{12} with methyl nicotinate at shorter reaction times is $HRu_3(\mu\text{-}1,2\text{-}NC_5H_3\text{-}5\text{-}CO_2Me)(CO)_{10}$ (**1**) (Figure 1(a), L = CO). The characterization of the product *via* IR and ^1H NMR is straight-forward, and the regiochemistry of the C–H addition is confirmed from the crystal structure of the PPh_3 substitution product $HRu_3(NC_5H_3\text{-}CO_2Me)$ $(CO)_9(PPh_3)$ (**2**) (Figure 2).

Thermally promoted substitution on (**1**) at 25–65°C in the presence of 2–3 equiv. of PPh_3 produces $HRu_3(NC_5H_3CO_2Me)(CO)_9(PPh_3)$ (**2**). The ^1H NMR spectra during the reaction show the presence of other hydride-containing compounds, but we were unable to isolate pure materials.

Slow reaction with PPh_3 over a period of days formed a species characterized by a hydride resonance at −8.10 (d, $J_{PH} = 19.1$ Hz), and a methoxy resonance at 3.96 (s) ppm; other hydride resonances, each attributed to a different compound, appeared at longer times and with larger excesses of PPh_3: −7.40 (t, 1H, $J_{PH} = 11.3$ Hz), −7.95 (dd, 1H, $J_{PH} = 17.7$, 8.6 Hz), and −13.85 (broad) ppm. These species have not been isolated or characterized in a pure state.

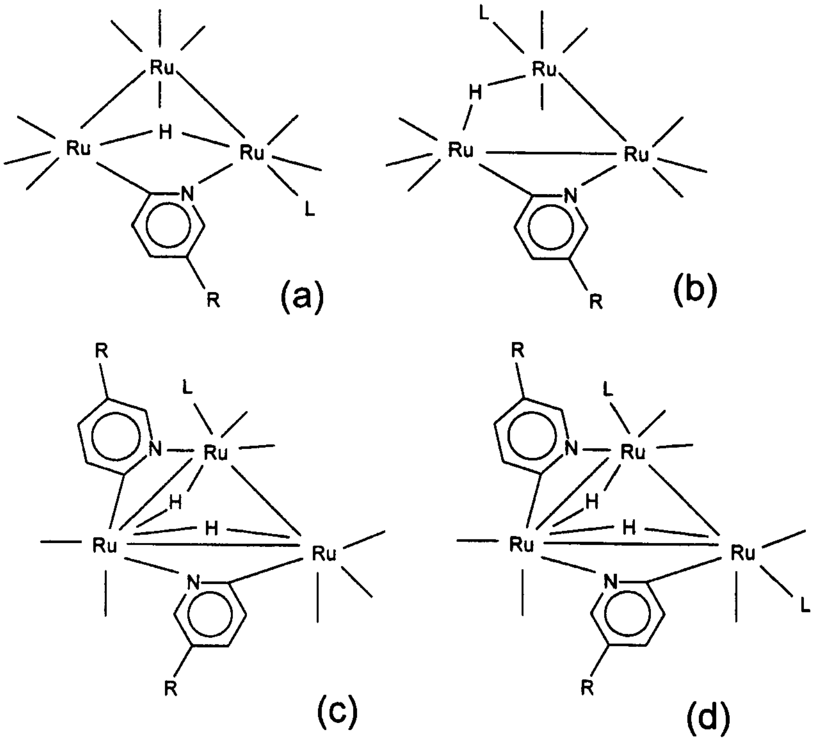

FIGURE 1 Structures of substituted $HRu_3(\mu\text{-}NC_5H_3R)(CO)_9L$ and $H_2Ru_3(\mu\text{-}NC_5H_3R)_2(CO)_8L$.

Description of the structure of $(\mu\text{-}H)Ru_3(\mu\text{-}\eta^2\text{-}NC_5H_3CO_2Me)(CO)_9(PPh_3)$ (**2**)

The crystal consists of discrete molecular units of $(\mu\text{-H})Ru_3(\mu\text{-}\eta^2\text{-}NC_5H_3CO_2Me)(CO)_9(PPh_3)$ which are mutually separated by typical van der Waals' distances. Each molecule has only C_1 symmetry and is therefore chiral; the crystal as a whole is a racemic mixture with molecules of each hand related by crystallographic symmetry elements. [In space group Pbca the defined molecule is related to molecules of the same chirality by 2_1 axes (along *a*, *b* and *c*) and to the enantiomeric form by symmetry elements of the second kind (an inversion center and by the *b*-, *c*-, and *a*-glide planes).] The defined molecule is illustrated in Figure 2. Selected interatomic distances are collected in Table IV, while interatomic angles are provided in Table V.

The molecular structure is based upon a triangular array of ruthenium atoms in which the interatomic distances (in increasing order) are Ru(1)–Ru(2) = 2.854(1), Ru(2)–Ru(3) = 2.861(1) and Ru(1)–Ru(2) = 2.910(1) Å.

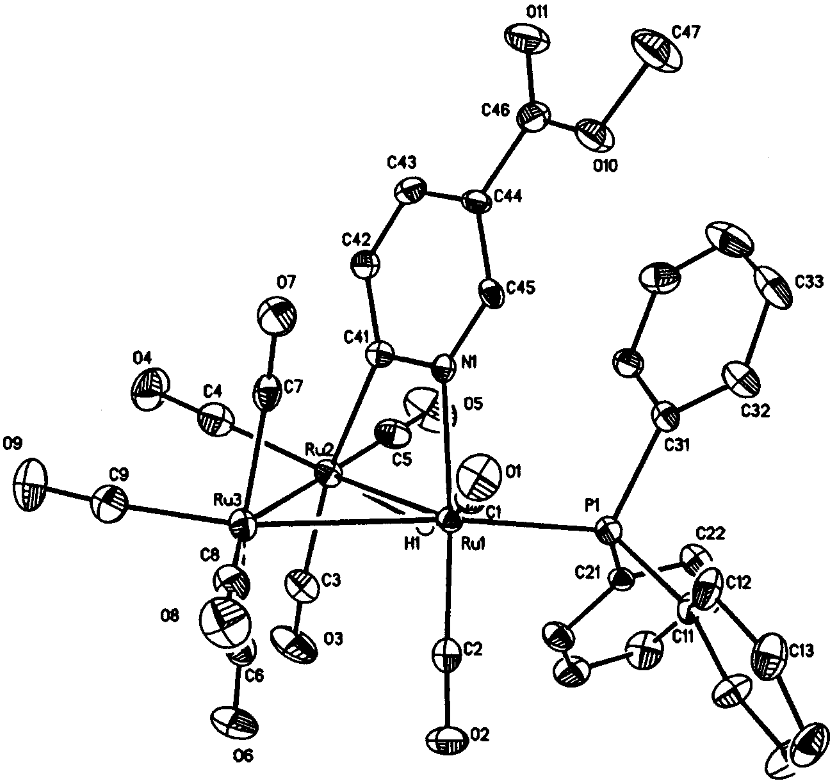

FIGURE 2 Labelling of atoms in (μ-H)Ru_3(μ-η^2-$NC_5H_3CO_2Me$)$(CO)_9$(PPh_3). All organic hydrogen atoms have been omitted. The hydride ligand, H(1), which was both located and refined, is shown artificially reduced. (ORTEP2 diagram, 30% probability ellipsoids.)

The longest of these is for that bond bridged by a di-equatorially-bridging hydride ligand. This ligand was located directly, and its positional parameters were refined, yielding Ru(1)–H(1) = 1.69(5) Å, Ru(2)–H(1) = 1.72(5) Å and ∠Ru(1)–H(1)–Ru(2) = 117.5(27)°. The non-bridged Ru–Ru bonds are quite close in value to those found in $Ru_3(CO)_{12}$ (Ru–Ru = 2.8512(4)–2.8595(4) Å; average value = 2.854 Å).[14] The expansion of the hydrido-bridged Ru–Ru bond is in good agreement with previous studies.[15–17] We also note that the presence of the di-equatorial hydride ligand causes displacement of the adjacent equatorial carbonyl ligands so that we observe the anomalously large *cis* angles Ru(2)–Ru(1)–P(1) = 111.5(1)° and Ru(1)–Ru(2)–C(5) = 113.0(3)°. These increases are very similar to those found in (μ-H)(H)$Os_3(CO)_{11}$, which has been compared to the more symmetrical isomorphous species, $Os_3(CO)_{12}$.[18] It is somewhat

TABLE IV Selected interatomic distances for $(\mu\text{-H})Ru_3(\mu\text{-}\eta^2\text{-}NC_5H_3CO_2Me)(CO)_9(PPh_3)$

Atoms	*Dist*, Å	*Atoms*	*Dist*, Å
Ru–Ru, Ru–H and Ru–P distances			
Ru(1)–Ru(2)	2.910(1)	Ru(1)–H(1)	1.69(5)
Ru(1)–Ru(3)	2.854(1)	Ru(2)–H(1)	1.72(5)
Ru(2)–Ru(3)	2.861(1)	Ru(1)–P(1)	2.365(2)
Ru–N and Ru–C distances to the methyl nicotinate ligand			
Ru(1)–N(1)	2.136(6)	Ru(2)–C(41)	2.088(7)
Ru–CO and C–O distances			
Ru(1)–C(1)	1.867(8)	C(1)–O(1)	1.144(9)
Ru(1)–C(2)	1.860(8)	C(2)–O(2)	1.149(10)
Ru(2)–C(3)	1.968(9)	C(3)–O(3)	1.113(11)
Ru(2)–C(4)	1.893(9)	C(4)–O(4)	1.148(11)
Ru(2)–C(5)	1.894(9)	C(5)–O(5)	1.135(11)
Ru(3)–C(6)	1.924(9)	C(6)–O(6)	1.144(10)
Ru(3)–C(7)	1.943(8)	C(7)–O(7)	1.133(10)
Ru(3)–C(8)	1.894(9)	C(8)–O(8)	1.147(11)
Ru(3)–C(9)	1.914(9)	C(9)–O(9)	1.148(11)
Distances within the methyl nicotinate ligand			
N(1)–C(41)	1.356(9)	C(44)–C(46)	1.486(11)
C(41)–C(42)	1.400(10)	C(46)–O(10)	1.308(11)
C(42)–C(43)	1.354(11)	C(46)–O(11)	1.211(11)
C(43)–C(44)	1.399(11)	O(10)–C(47)	1.433(9)
C(44)–C(45)	1.366(11)		
C(45)–N(1)	1.350(9)		
P–C distances			
P(1)–C(11)	1.833(8)	P(1)–C(31)	1.824(8)
P(1)–C(21)	1.833(7)		
C–C distances within phenyl rings			
C(11)–C(12)	1.383(11)	C(21)–C(22)	1.381(10)
C(12)–C(13)	1.372(13)	C(22)–C(23)	1.388(11)
C(13)–C(14)	1.366(13)	C(23)–C(24)	1.355(14)
C(14)–C(15)	1.366(14)	C(24)–C(25)	1.374(13)
C(15)–C(16)	1.370(13)	C(25)–C(26)	1.371(12)
C(16)–C(11)	1.383(11)	C(26)–C(21)	1.385(10)
C(31)–C(32)	1.387(11)	C(34)–C(35)	1.356(15)
C(32)–C(33)	1.393(14)	C(35)–C(36)	1.368(13)
C(33)–C(34)	1.361(18)	C(36)–C(31)	1.383(12)

surprising that the bulky equatorial triphenylphosphine ligand on Ru(1) causes little additional angular dissymmetry.

The methyl nicotinate ligand spans Ru(1) and Ru(2) with metal–ligand bond lengths of Ru(1)–N(1) = 2.136(6) Å and Ru(2)–C(41) = 2.088(7) Å. The C–C bond lengths within the six-membered heterocyclic ring appear to show a pattern of alternation (thus we have, cyclically, C(45)–N(1) = 1.350(9) Å and N(1)–C(41) = 1.356(9) Å, followed by a pattern of long and short C–C bonds, *viz.*, C(41)–C(42) = 1.400(10) Å,

TABLE V Selected interatomic angles for $(\mu\text{-H})Ru_3(\mu\text{-}\eta^2\text{-}NC_5H_3CO_2Me)(CO)_9(PPh_3)$

Atoms	*Angle* (°)	*Atoms*	*Angle* (°)
Ru–Ru–Ru, Ru–Ru–H and Ru–H–Ru angles			
Ru(2)–Ru(1)–Ru(3)	59.5(1)	Ru(3)–Ru(1)–H(1)	84.9(17)
Ru(1)–Ru(2)–Ru(3)	59.3(1)	Ru(3)–Ru(2)–H(1)	84.2(16)
Ru(2)–Ru(3)–Ru(1)	61.2(1)	Ru(1)–H(1)–Ru(2)	117.5(27)
Angels around Ru(1) and Ru(2), arranged side-by-side so as to show the similarity in their coordination geometry			
Ru(2)–Ru(1)–N(1)	68.7(2)	Ru(1)–Ru(2)–C(41)	68.0(2)
Ru(2)–Ru(1)–P(1)	111.5(1)	Ru(1)–Ru(2)–C(5)	113.0(3)
Ru(2)–Ru(1)–C(1)	142.4(2)	Ru(1)–Ru(2)–C(4)	140.8(3)
Ru(2)–Ru(1)–C(2)	107.5(2)	Ru(1)–Ru(2)–C(3)	107.1(2)
Ru(3)–Ru(1)–N(1)	90.1(1)	Ru(3)–Ru(2)–C(41)	87.5(2)
Ru(3)–Ru(1)–P(1)	168.1(1)	Ru(3)–Ru(2)–C(5)	170.7(2)
Ru(3)–Ru(1)–C(1)	91.1(2)	Ru(3)–Ru(2)–C(4)	86.8(3)
Ru(3)–Ru(1)–C(2)	86.1(2)	Ru(3)–Ru(2)–C(3)	96.8(2)
N(1)–Ru(1)–P(1)	93.5(1)	C(41)–Ru(2)–C(5)	84.4(3)
N(1)–Ru(1)–C(1)	90.3(3)	C(41)–Ru(2)–C(4)	93.5(3)
N(1)–Ru(1)–C(2)	175.7(3)	C(41)–Ru(2)–C(3)	170.7(3)
P(1)–Ru(1)–C(1)	100.2(2)	C(5)–Ru(2)–C(4)	98.4(4)
P(1)–Ru(1)–C(2)	89.7(2)	C(5)–Ru(2)–C(3)	90.6(3)
C(1)–Ru(1)–C(2)	91.9(3)	C(4)–Ru(2)–C(3)	95.0(4)
H(1)–Ru(1)–C(1)	173.7(17)	H(1)–Ru(2)–C(4)	170.9(16)
Angles around Ru(3)			
Ru(1)–Ru(3)–C(6)	90.9(3)	Ru(2)–Ru(3)–C(6)	82.1(2)
Ru(1)–Ru(3)–C(7)	80.2(2)	Ru(2)–Ru(3)–C(7)	90.6(2)
Ru(1)–Ru(3)–C(8)	97.3(2)	Ru(2)–Ru(3)–C(8)	157.6(2)
Ru(1)–Ru(3)–C(9)	162.6(3)	Ru(2)–Ru(3)–C(9)	102.4(3)
C(6)–Ru(3)–C(7)	170.5(3)	C(7)–Ru(3)–C(8)	91.8(3)
C(6)–Ru(3)–C(8)	92.7(3)	C(7)–Ru(3)–C(9)	95.3(4)
C(6)–Ru(3)–C(9)	92.2(4)	C(8)–Ru(3)–C(9)	99.6(4)
Ru–C–O angles			
Ru(1)–C(1)–O(1)	174.4(7)	Ru(3)–C(6)–O(6)	174.2(7)
Ru(1)–C(2)–O(2)	178.1(7)	Ru(3)–C(7)–O(7)	173.0(7)
Ru(2)–C(3)–O(3)	172.6(8)	Ru(3)–C(8)–O(8)	179.3(7)
Ru(2)–C(4)–O(4)	177.6(8)	Ru(3)–C(9)–O(9)	175.5(8)
Ru(2)–C(5)–O(5)	177.7(7)		
Angles involving the methyl nicotinate moiety			
Ru(1)–N(1)–C(41)	108.9(4)	Ru(2)–C(41)–N(1)	114.1(5)
Ru(1)–N(1)–C(45)	130.2(5)	Ru(2)–C(41)–C(42)	127.4(5)
C(41)–N(1)–C(45)	120.9(6)	N(1)–C(41)–C(42)	118.3(6)
N(1)–C(45)–C(44)	122.1(7)	C(41)–C(42)–C(43)	121.0(7)
C(45)–C(44)–C(43)	117.9(7)	C(42)–C(43)–C(44)	119.9(7)
C(45)–C(44)–C(46)	121.4(7)	C(43)–C(44)–C(46)	120.7(7)
C(44)–C(46)–O(10)	114.1(8)	C(44)–C(46)–O(11)	122.0(8)
C(46)–O(10)–C(47)	115.4(7)	O(10)–C(46)–O(11)	124.0(8)
Angles around P(1)			
Ru(1)–P(1)–C(11)	112.8(2)	C(11)–P(1)–C(21)	103.1(3)
Ru(1)–P(1)–C(21)	117.4(2)	C(11)–P(1)–C(31)	107.3(3)
Ru(1)–P(1)–C(31)	113.5(2)	C(21)–P(1)–C(31)	101.5(3)

C(42)–C(43) = 1.354(11) Å, C(43)–C(44) = 1.399(11) Å, C(44)–C(45) = 1.366(11) Å. While this pattern is on the borderline of statistical significance (the two "long" bonds average 1.400 ± 0.001 Å and the two "short" bonds average 1.360 ± 0.008 Å),[‡] these results are rendered more meaningful insofar as they contrast sharply with those for the phenyl groups of the PPh_3 ligand, in which the "observed" C–C bond lengths decrease as a function of distance from the ipso carbon. (The "bond shortening" in these phenyl rings is an artifact, caused by the increasingly large amplitudes of vibration of atoms as a function of distance from the centroid of the molecule.) The methyl carboxylate portion of the molecule is clearly defined by a short C=O bond (C(46)–O(11) = 1.211(11) Å) and longer C–O distances for the C–O–Me system (C(46)–O(10) = 1.308(11) Å and O(10)–C(47) = 1.433(9) Å).

The Ru–CO distances show systematic variations according to their chemical environment. Thus, the Ru–CO bond Ru(2)–C(3) = 1.968(9) Å is the longest, due to the *trans*-lengthening influence of the σ-bonded carbon atom C(41).[19] [The angle C(41)–Ru(2)–C(3) is 170.7(3)°.] Note that the nitrogen donor atom N(1) does *not* show a similar effect. In fact, the carbonyl ligand *trans* to N(1) (with angle N(1)–Ru(1)–C(2) = 175.7(3)°) has the *shortest* Ru–CO bond length of all, Ru(1)–C(2) = 1.860(8) Å. The mutually *trans* ($\angle$C(6)–Ru(3)–C(7) = 170.5(3)°) carbonyl groups on Ru(3) are also associated with long Ru–CO distances, as a result of competition for back-donation of electron density from the metal atom; here we have Ru(3)–C(6) = 1.924(9) Å and Ru(3)–C(7) = 1.943(8) Å. All other Ru–CO distances are within the range 1.867(8) to 1.914(9) Å.

The crystal structures of $HRu_3(\mu\text{-}NC_5H_4)(CO)_9(PPh_3)$[20] and $HRu_3(\mu\text{-}NC_5H_4)(CO)_9(P\text{-}i\text{-}Pr_3)$[21] have been previously reported, as well as that of the parent $HRu_3(\mu\text{-}NC_5H_4)(CO)_{10}$.[21] The structure of $HRu_3(\mu\text{-}NC_5H_4)(CO)_9(PPh_3)$, prepared by thermally induced substitution, is entirely analogous to that of (**2**), with substitution on the N-ligated Ru atom in an equatorial position. However, the $P\text{-}i\text{-}Pr_3$ derivative adopts a different structure (Figure 1(b), L = $P\text{-}i\text{-}Pr_3$) with the phosphine bonded to the Ru atom which is not bridged by the pyridyl ligand and also with the hydride bridging a different Ru–Ru edge. At this time it is not possible to account for the substitution geometry in this class of clusters. However, we see no

---

[‡] Esd's on the average values are calculated by the 'internal scatter' formula:

$$\sigma(\text{av}) = \left[\sum_{i=1}^{i=N}(\bar{\chi} - \chi_i)^2/(N-1)\right]^{1/2}$$

where $\bar{\chi}$ is the average value and χ_i is the *i*th of the N equivalent values.

evidence that the presence of the ester functionality affects either the activation of the pyridine ring or the carbonyl substitution behavior.

$H_2Ru_3(\mu\text{-}NC_5H_3CO_2Me)_2(CO)_{8-n}(PPh_3)_n$ $(n = 0, 1, 2)$

Thermal reaction of methyl nicotinate with $Ru_3(CO)_{12}$ also produced the (bis)nicotinyl complex $H_2Ru_3(NC_5H_3CO_2Me)_2(CO)_8$ (**3**) (Figure 1(c), L = CO). Again, the spectroscopic characterization is entirely analogous to the data for $H_2Ru_3(NC_5H_4)_2(CO)_8$, previously reported. The regiochemistry of the C–H addition is shown by the crystal structure of the phosphine-substituted derivative (*vide infra*).

Ligand substitution on bis(pyridyl) clusters has not been previously reported. Clusters of the series $H_2Ru_3(NC_5H_3CO_2Me)_2(CO)_{8-n}(PPh_3)_n$ ($n = 1$ or 2), were prepared using the same procedures as described above. Formation of $H_2Ru_3(NC_5H_3CO_2Me)_2(CO)_7(PPh_3)$ (**4**) was accomplished by thermal substitution; only one product is observed (Figure 1 (c), L = PPh_3). The solid state structure was established by single crystal X-ray diffraction. The spectroscopic data are consistent with this structure in solution.

Description of the structure of $(\mu\text{-}H)_2Ru_3(\mu\text{-}\eta^2\text{-}NC_5H_3CO_2Me)_2(CO)_7(PPh_3)$ (**4**)

The crystal is composed of discrete molecular units of $(\mu\text{-H})_2Ru_3(\mu\text{-}\eta^2\text{-}NC_5H_3CO_2Me)_2(CO)_7(PPh_3)$, which are separated by normal van der Waals' distances. The molecule has no symmetry (point group C_1) and the crystal is an ordered racemic mixture of the two enantiomeric forms. [In space group $P2_1/c$, the defined molecule and that related to it by a 2_1 operation define one enantiomeric form; the molecules related to these by inversion centers and *c*-glide planes define the alternative enantiomer.] The molecule is illustrated in Figure 3. Selected interatomic distances are collected in Table VI. This structural study is not as accurate as the previous one, due to substantially weaker diffraction data. Our discussion will be appropriately less detailed.

This molecule also contains a central Ru_3 triangle, within which Ru(1)–Ru(2) = 2.924(2) Å, Ru(1)–Ru(3) = 2.914(2) Å and Ru(2)–Ru(3) = 2.846(2) Å. The two hydride ligands span the two longer Ru–Ru bonds. These hydride ligands were located on a difference-Fourier map yielding distances of Ru(1)–H(1) = 1.62 Å and H(1)–Ru(3) = 1.85 Å with ∠Ru(1)–H(1)–Ru(3) = 114°; Ru(1)–H(2) = 1.45 Å, H(2)–Ru(2) = 1.94 Å and ∠Ru(1)–H(2)–Ru(2) = 118°. Atom H(1) is situated *trans* to both C(1) and C(7) (∠C(1)–Ru(1)–H(1) = 167°, ∠C(7)–Ru(3)–H(1) = 172°), while H(2) is in a location *trans* to both C(2) and C(4) (∠C(2)–Ru(1)–H(2) = 169°,

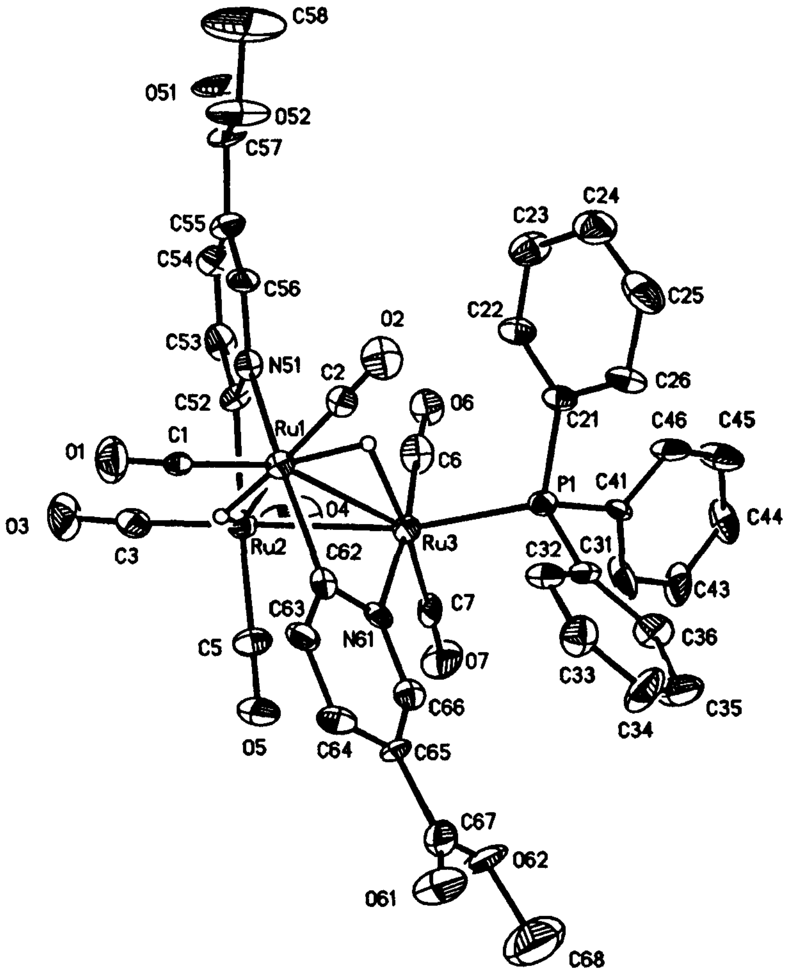

FIGURE 3 Labelling of atoms in $(\mu\text{-H})_2\text{Ru}_3(\mu\text{-}\eta^2\text{-NC}_5\text{H}_3\text{CO}_2\text{Me})_2(\text{CO})_7(\text{PPh}_3)$. All organic hydrogen atoms have been omitted. The hydride ligands are shown in the positions determined from a difference-Fourier synthesis. (ORTEP2 diagram with 30% probability ellipsoids.)

$\angle$C(4)–Ru(2)–H(2) = 167°). Attempts to refine the positions of these hydrogen atoms were unsuccessful – the positions of the atoms oscillated – so the parameters above are derived from unrefined 'peak positions'.

The two methyl nicotinate ligands each span a Ru–Ru bond in a diaxial manner. The first spans the Ru(1)–Ru(2) bond with Ru(1)–N(51) = 2.122(13) Å and Ru(2)–C(52) = 2.100(16) Å. The second spans the Ru(1)–Ru(3) bond with Ru(1)–C(62) = 2.053(16) Å and Ru(3)–N(61) = 2.129(14) Å. These ligands have a relative orientation such that Ru(1) is

TABLE VI Selected interatomic distances for $(\mu\text{-H})_2\mathrm{Ru}_3(\mu\text{-}\eta^2\text{-NC}_5\mathrm{H}_3\mathrm{CO}_2\mathrm{Me})(\mathrm{CO})_7(\mathrm{PPh}_3)$

Atoms	*Dist*, Å	*Atoms*	*Dist*, Å
Ru–Ru, Ru–P and Ru–H (from difference-Fourier map) distances			
Ru(1)–Ru(2)	2.924(2)	Ru(1)–H(1)	1.62
Ru(1)–Ru(3)	2.914(2)	Ru(1)–H(2)	1.45
Ru(2)–Ru(3)	2.846(2)	Ru(2)–H(2)	1.94
Ru(3)–P(1)	2.379(4)	Ru(3)–H(1)	1.85
Ru–N and Ru–C distances to the methyl nicotinate ligands			
Ru(1)–N(51)	2.122(13)	Ru(2)–C(52)	2.100(16)
Ru(3)–N(61)	2.129(14)	Ru(1)–C(62)	2.053(16)
Ru–CO and C–O bond lengths			
Ru(1)–C(1)	1.847(17)	C(1)–O(1)	1.166(22)
Ru(1)–C(2)	1.835(16)	C(2)–O(2)	1.167(19)
Ru(2)–C(3)	1.825(18)	C(3)–O(3)	1.193(22)
Ru(2)–C(4)	1.874(18)	C(4)–O(4)	1.159(21)
Ru(2)–C(5)	1.945(19)	C(5)–O(5)	1.129(22)
Ru(3)–C(6)	1.804(18)	C(6)–O(6)	1.184(21)
Ru(3)–C(7)	1.881(19)	C(7)–O(7)	1.158(23)
Distances within the methyl nicotinate ligands			
N(51)–C(52)	1.397(20)	N(61)–C(62)	1.353(22)
C(52)–C(53)	1.382(24)	C(62)–C(63)	1.387(25)
C(53)–C(54)	1.367(20)	C(63)–C(64)	1.340(27)
C(54)–C(55)	1.449(27)	C(64)–C(65)	1.376(29)
C(55)–C(56)	1.364(27)	C(65)–C(66)	1.398(28)
C(56)–N(51)	1.369(22)	C(66)–N(61)	1.324(23)
C(55)–C(57)	1.459(28)	C(65)–C(67)	1.491(33)
C(57)–O(51)	1.191(30)	C(67)–O(61)	1.224(33)
C(57)–O(52)	1.348(30)	C(67)–O(62)	1.274(32)
O(52)–C(58)	1.385(26)	O(62)–C(68)	1.498(28)
P–C distances			
P(1)–C(21)	1.806(17)	P(1)–C(41)	1.816(18)
P(1)–C(31)	1.854(22)		

linked to atoms N(51) and C(62) in mutually *trans* positions (∠N(51)–Ru(1)–C(62) = 161.5(6)°).

The longest Ru–CO bond length (Ru(2)–C(5) = 1.945(19) Å) is for the carbonyl ligand *trans* to the σ-bonded carbon of a nicotinate ligand (∠C(5)–Ru(2)–C(52) = 171.6(7)°) and the shortest (Ru(3)–C(6) = 1.804(18) Å) is for the carbonyl ligand *trans* to the donor nitrogen atom on the other nicotinate ligand (∠C(6)–Ru(3)–N(61) = 172.5(7)°). All other Ru–CO bond lengths are in the range 1.825(18) to 1.881(19) Å.

Finally we note that the PPh_3 ligand occupies an equatorial site on Ru(3) with Ru(3)–P(1) = 2.379(4) Å.

The structure of $\mathrm{H}_2\mathrm{Ru}_3(\mu\text{-NC}_5\mathrm{H}_4)_2(\mathrm{CO})_8$ was reported after we had completed the structure determination.[22] This structure contained disordered pyridyl ligands and so comparison of the *trans* effects of the C- and

N-donor atoms of the pyridyl ligands cannot be made. Phosphine substitution causes no significant structural changes.

Further substitution on (**4**) could not be effected by heating. However, treatment of (**3**) with two equiv. trimethylamine-N-oxide and two equiv. of PPh_3 in THF/acetonitrile solution or (**4**) with one equiv. of these reagents gave $H_2Ru_3(\mu\text{-}NC_5H_3CO_2Me)_2(CO)_6(PPh_3)_2$ (**5**), in addition to (**4**) and two other products. The proposed structure for (**5**) is shown in Figure 1(d). The hydride resonances are similar in chemical shifts to those of $(\mu\text{-}H)_2Ru_3(\mu\text{-}\eta^2\text{-}NC_5H_3CO_2Me)_2(CO)_7(PPh_3)$ and additional ^{31}P coupling to the hydrides and between the two ^{31}P nuclei consistent with PPh_3 substitution *cis* to the second hydride and *trans* to the site occupied by the PPh_3 ligand of (**2**) (^1H NMR: −12.55 (dd, 1H, $J_{PH} = 2.0$, 12.0 Hz), −11.79 (dd, 1H, $J_{PH} = 1.6$, 10.8 Hz), 3.75 (s, 3H), 3.93 (s, 3H), 6.96 (d, 1H, $J_{HH} = 4.0$ Hz), 7.04 (d, 1H, $J_{HH} = 4.0$ Hz), 7.2 (m, 30H), 7.7 (s, 3H), 8.4 (s, 3H) ppm. ^{31}P NMR: 32.7 (d, 1P, $J_{PP} = 16.0$ Hz), 39.2 (d, 1P, $J_{PP} = 16.0$ Hz) ppm).

Regiochemistry of ligand substitution

For both nicotinyl clusters examined, the first (thermally induced) substitution occurs on the N-ligated Ru atom rather than the C-ligated one. The longer Ru–CO bond lengths *trans* to C, rather than N, are evidence of greater *trans* influence for C, consistent with the greater *trans* influence in square-planar complexes of phenyl compared with pyridine. Clearly, the substitutional preference is not due to the *trans* influence, a ground state effect. We presume that the preferred substitutional pattern arises from greater *cis* labilization of the N-donor atom, compared with the C-donor. While data comparing labilization by aryl *vs.* pyridine are not available, pyridine is known to be a *cis* labilizing ligand.[23] If this accounts for the substitutional pattern, then it may be assumed that aryl ligands are poorer *cis* labilizers than pyridine. This is consistent with the general trend that the order of ligands in the *trans* effect for square-planar complexes (Ph- > py) is opposite to that of *cis* labilization in octahedral complexes.

Phosphine substitution on a related cluster $HOs_3(\mu\text{-}\eta^2\text{-Cyclo-C}{=}\,NCH_2CH_2CH_2)(CO)_{10}$ gave a 4 : 1 mixture of C- to N-substitution products.[24] Intermetallic migration also is a possible complicating factor in this case, so the product distribution may be thermodynamically determined.

Supplementary Material Available

Complete tables of interatomic distances and angles, anisotropic thermal parameters and calculated positions for the hydrogen atoms for each structural study are available from M.R.C.

Acknowledgments

Purchase of the Siemens R3m/V diffractometer was made possible by Grant 89-13733 from the Chemical Instrumentation Program of the National Science Foundation. This work was funded by a grant from the National Science Foundation (CHE9213695) to J.B.K.

References

[1] M.I. Bruce, M.P. Cifuentes and M.G. Humphrey, *Polyhedron* **10**, 277 (1991).

[2] R. Zoet, G. van Koten, K. Vrieze, J. Jansen, K. Goubitz and C.H. Stam, *Organometallics* **7**, 1565 (1988).

[3] R.H. Fish, T. Kim, J.L. Stewart, J.H. Bushweller, R.K. Rosen and J.W. Dupon, *Organometallics* **5**, 2193 (1986).

[4] A. Eisenstadt, C.M. Giandomenico, M.F. Frederick and R.M. Laine, *Organometallics* **4**, 2033 (1985).

[5] E.C. Constable, *Polyhedron* **3**, 1037 (1984).

[6] G.A. Foulds, B.F.G. Johnson and J. Lewis, *J. Organomet. Chem.* **294**, 123 (1985).

[7] (a) M.I. Bruce, M.G. Humphrey, M.R. Snow, E.R.T. Tiekink and R.C. Wallis, *J. Organomet. Chem.* **314**, 311 (1986); (b) J.A. Van Doorn and P.W.N.M. Van Leeuwen, *J. Organomet. Chem.* **222**, 299 (1981).

[8] E.J. Moore, W.R. Pretzer, T.J. O'Connell, J. Harris, L. LaBounty, L. Chou and S.S. Grimmer, *J. Am. Chem. Soc.* **114**, 5888 (1992).

[9] J.L. Dawes and J.D. Holmes, *Inorg. Nucl. Chem. Lett.* **7**, 847 (1971).

[10] M.R. Churchill, R.A. Lashewycz and F.J. Rotella, *Inorg. Chem.* **16**, 265 (1977).

[11] (a) *Siemens SHELXTL PLUS Manual*, 2nd edn., Siemens Analytical Instruments, Madison, WI, 1990; (b) G.M. Sheldrick, *SHELXTL PLUS* (*Release 4.11 VMS*). An integrated system for solving, refining and displaying crystal structures from diffraction data. For Nicolet R3m/V; University of Göttingen, Germany, 1987.

[12] *International Tables for X-Ray Crystallography*, Kynoch Press, Birmingham, England, 1974, Vol. 4, pp. 99–101 and 149–150.

[13] M.R. Churchill, *Inorg. Chem.* **12**, 1213 (1973).

[14] M.R. Churchill, F.J. Hollander and J.P. Hutchinson, *Inorg. Chem.* **16**, 2655 (1977).

[15] M.R. Churchill, B.G. DeBoer and F.J. Rotella, *Inorg. Chem.* **15**, 1843 (1976) (see especially, discussion on pp. 1848–1852).

[16] M.R. Churchill, *Adv. Chem. Ser.* **167**, 36 (1978).

[17] R.G. Teller and R. Bau, *Structure and Bonding* **44**, 1 (1981).

[18] M.R. Churchill and B.G. DeBoer, *Inorg. Chem.* **16**, 878 (1977).

[19] M.R. Churchill, "*Perspectives in Structural Chemistry*", Edited by J.D. Dunitz and J.A. Ibers, John Wiley & Sons, 1970, Vol. 3, pp. 91–164 (see especially, Section XA, pp. 151–153).

[20] M.P. Cifuentes, M.G. Humphrey, B.W. Skelton and A.H. White, *J. Organometal. Chem.* **466**, 211 (1994).

[21] D. Ellis and L.J. Farrugia, *J. Cluster Science* **7**, 71 (1996).

[22] M.P. Cifuentes, M.G. Humphrey, B.W. Skelton and A.H. White, *J. Organomet. Chem.* **513**, 201 (1996).

[23] J.D. Atwood and T.L. Brown, *J. Am. Chem. Soc.* **98**, 3160 (1976).

[24] M. Day, D. Espitia, K.I. Hardcastle, S.E. Kabir, E. Rosenberg, R. Gobetto, L. Milone and D. Osella, *Organometallics* **10**, 3550 (1991).